Semi-analytical 6D model of space charge force for dense electron bunches with a large energy spread

Gwenaël Fubiani[1], Gerald Dugan[2], Wim Leemans, Eric Esarey and Jean Louis Bobin[3]

Center for Beam Physics, Ernest Orlando Lawrence Berkeley National Laboratory,University of California, Berkeley CA 94720

Abstract. Laser driven accelerators are capable of producing multi nC, multi MeV electron beams with transverse and longitudinal sizes on the order of microns. To investigate the transport of such electron bunches, a fast and fully relativistic space charge code which can handle beams with arbitrarily large energy spread has been developed. A 6-D macroparticle model for the beam is used to calculate the space charge fields at each time step. The collection of macroparticles is divided into longitudinal momentum bins, each with a small spread in relative momentum. The macroparticle distribution in each momentum bin is decomposed into ellipsoidal shells in position space. For each shell, an analytical expression for the electrostatic force in the bin rest frame is used. The total space charge force acting on one macroparticle in the lab frame is then the vector sum of the Lorentz-transformed forces from all the momentum bins. We have used this code to study the evolution of typical beams emerging from the plasma in the two most popular schemes, i.e., the self-modulated laser-wakefield-accelerator, where the laser pulse size is many times the plasma wavelength ($L \gg \lambda_p$), and the colliding pulse laser-wakefield-accelerator regime where $L \sim \lambda_p$ and two counterpropagationg laser pulses are used to inject electrons into the wakefield.

INTRODUCTION

The self-modulated laser-wakefield-accelerator (SMLWFA) accelerator [1] relies on an instability to inject electrons into the plasma wakefield via wavebreaking. Because the electrons are injected into the wakefield buckets in an uncontrolled manner, the resulting bunch has a large energy spread, characterized by an exponential distribution in energy with a mean of ~ 4 MeV. The bunch has a high charge $\sim 2-4$ nC, with typical transverse dimensions ~ 10 μm and bunch half length ~ 10 μm, giving a high number density $\sim 2.5 \times 10^{19}$ cm^{-3}.

Optical injection, such as in the colliding pulse injector (CPI) scheme [2], allows the production of electron bunches of small relative energy spread. CPI uses two to three short laser pulses of length L comparable to the plasma wavelength λ_p. The drive pulse at greatest normalized intensity ($a_0 \sim 1$) generates the wake, and the beating of the

---

[1] Also at University of Paris XI, France

[2] Laboratory of Elementary Particle Physics, Cornell University, Ithaca, NY 14853

[3] University Pierre et Marie Curie, France

backward pulse with the drive pulse (or a third pulse) injects electrons with a small phase spread into the wakefield. This scheme offers detailed control of the injection process, and since $L \lesssim \lambda_p$, Raman and self-modulation instabilities will be suppressed.

The resulting electron bunches carry a charge ~ 10 pC, with an average energy up to ~ 10 MeV, and a relative energy spread of $1-5\%$. The bunch typical transverse dimensions are ~ 10 μm, and the bunch half length is ~ 2.5 μm, corresponding to a number density of $\sim 2.5 \times 10^{17}$ cm^{-3}. This is two orders of magnitude smaller than in the self-modulated regime, but the longitudinal quality of the beam is much better because of the small relative energy spread.

The dynamics of MeV scale electron beams with such high charge densities is expected to be dominated by space charge effects [3]. The total electrostatic potential energy per electron, Φ, in a spherical bunch of radius R, containing N electrons of charge e and mass m, is $\Phi \sim mc^2 N r_e/(10R)$. For $Ne = 5$ nC and $R = 5$ μm, the potential energy per electron is about 0.9 MeV. This will be transformed into kinetic energy as the beam evolves in time, resulting in a large space charge induced relative energy spread and substantial transverse emittance growth.

A code which can handle properly the space charge blowout of such electron beams must be able to treat bunches with a large relative energy spread. Currently two main types of numerical codes exist:

- Typical accelerator physics codes assume that the electron bunch has a small relative energy spread $< 1\%$. In this case there is a single frame in which all beam particles are non-relativistic, which simplifies the calculation of the electromagnetic self field.
- Particle-in-cell (PIC) codes solve Maxwell's equations on a grid. This method can properly cope with a large relative energy spread in the beam but is very slow.

This paper discusses a rapid and innovative method for the calculation of space charge effects, which is capable of handling beams with an arbitrary energy distribution. As discussed below, the method is very general, only making certain assumptions about the position space ellipsoidal symmetry properties of the charge distribution. In this paper, we only consider evolution of the beam in the absence of external forces, and, in order to obtain simple analytical expressions for the space charge force, specialize to the case of charge distributions with radial symmetry about the axis of propagation.

STRUCTURE OF THE CODE

The 6D beam distribution function is represented numerically as a collection of macroparticles. The phase space coordinates of these macroparticles evolve under the influence of the collective space charge forces. To compute these space charge forces, we divide the range of longitudinal momenta spanned by the beam into a series of bins. Each bin has a normalized longitudinal momentum width $\Delta u_z = \Delta p_z/(mc) \ll 1$. Consequently, in the rest frame of each bin, the macroparticles within that bin are non-relativistic, and the space charge forces in that frame may be computed from the electrostatic field of the macroparticle charge distribution.

The macroparticle charge distribution is modeled as a series of concentric ellipsoidal shells. The parameters of these ellipsoidal shells, such as the rms radii, the density and the average position, are obtained by statistical calculations over the selected macroparticles. Analytical expressions are used for the electrostatic field for each ellipsoidal shell [4], which allow for writing a fast computational algorithm. The total electrostatic field due to the macroparticles is given by the sum over the ellipsoidal shells.

To calculate the force on a given macroparticle at each time step, we iterate through each momentum bin, and, from the electrostatic fields, calculate the space charge force on that macroparticle in the rest frame of that bin. We then transform the space charge force into the lab frame. The total force on the macroparticle is the vector sum of the Lorentz-transformed space charge forces due to all the momentum bins. This procedure is repeated for each macroparticle, giving all the forces needed to evolve the macroparticle distribution to the next time step.

Note that the binning by momentum, and the calculation of the ellipsoid parameters characterizing the macroparticle charge distribution associated with that bin, is done at every time step.

Adaptive longitudinal momentum grid

In order to be able to approximate the space charge fields as purely electrostatic, the collection of charges generating these fields must be non-relativistic in their common rest frame. Such an approximation requires that the normalized momentum spread in the rest frame be small, that is $\Delta p_{\rm cm}/(mc) = \Delta u_{\rm cm} = \eta \ll 1$.
This condition is achieved in the code by using an adaptive binning technique to break the longitudinal momentum distribution up into bins (the transverse momentum spread is small because of the small angular spread in the beam). The bin width requirement in terms of laboratory longitudinal (z) momentum, for a laboratory momentum u_{z_k} in bin k, is

$$\Delta u_z = u_{z_{k+1}} - u_{z_k} = \eta \sqrt{1+u_{z_k}^2}.$$

In the limiting case $\eta \ll 1$ one has,

$$\frac{du_z(k)}{dk} \sim \eta \sqrt{1+u_z^2}.$$

Hence, the longitudinal momentum bins are defined by

$$u_{z_k} = \sinh\left(\eta + k\ \sinh^{-1} u_{z_0}\right).$$

The bin index for a given momentum u_z is

$$k = \left\lfloor \frac{\sinh^{-1} u_z - \sinh^{-1} u_{z_0}}{\eta} \right\rfloor.$$

Note that u_{z_0} is taken as the lowest momentum of the distribution function: it defines the first bin.

Total force calculations

For the macroparticles in momentum bin k, we compute in the laboratory frame the transverse (a_{1k} and a_{2k} along x and y) and longitudinal (a_{3k} along the coordinate z) rms sizes of the bunch, and the mean longitudinal position of the bunch ($\langle z \rangle_k$). As noted above, radial symmetry is assumed , so that $a_{1k} = a_{2k} \equiv a_k$, in order to be able to use a simple analytical solution for the fields.

The quantities a_k and a_{3k} define an ellipsoid which has the shape of the macroparticle distribution. This ellipsoid is decomposed into a number of concentric ellipsoidal shells. The inner boundary of shell s_k is designated $m_0(s_k)\, a_k$ radially, and $m_0(s_k) a_{3k}$ longitudinally; the outer boundary is $m_1(s_k) a_k$ radially, and $m_1(s_k) a_{3k}$ longitudinally. The numbers $m_0(s_k)$ and $m_1(s_k)$, which range from 0 to μ_m (maximum ellipsoidal coordinate of the distribution function $\mu^2 = (x^2+y^2)/a_k^2 + \left(z - \langle z \rangle_k\right)^2 / a_{3k}^2$), are chosen such that the volume of each of the ellipsoidal shells is the same. The density of macroparticles within shell s_k, ρ_{s_k}, is calculated numerically from the macroparticle distribution.

The electromagnetic force per unit charge, produced by an ellipsoidal shell, acting at the coordinate $\{x,y,z\}$ in the laboratory frame, is given by,

$$\begin{aligned} F_x^{sh}(x,y,z) &= \frac{x}{\gamma_k} \frac{\rho_{s_k}}{2\varepsilon_0} a_k^2 a_{3_k} A_{s_k}(u_{1_k}(x,y,z), u_{0_k}(x,y,z)), \\ F_z^{sh}(x,y,z) &= \left(z - \langle z \rangle_k\right) \gamma_k \frac{\rho_{s_k}}{2\varepsilon_0} a_k^2 a_{3_k} A_{3_{s_k}}(u_{1_k}(x,y,z), u_{0_k}(x,y,z)), \end{aligned}$$

in which A_{s_k} ($A_{3_{s_k}}$) is the transverse (longitudinal) space charge coeficient, and γ_k is the relativistic factor of the kth bin. The space charge coefficients are

$$A_{s_k}(u_{1_k}, u_{0_k}) = f_k(u_{0_k}) - f_k(u_{1_k}),\ A_{3_{s_k}}(u_{1_k}, u_{0_k}) = g_k(u_{0_k}) - g_k(u_{1_k}),$$

with

$$f_k(u) = \left(a_k^2 - \gamma_k^2 a_{3_k}^2\right)^{-1} \left\{ \frac{\sqrt{\gamma_k^2 a_{3_k}^2 + u}}{a_k^2 + u} + \frac{\tan^{-1}\left[\sqrt{\frac{\gamma_k^2 a_{3_k}^2 + u}{a_k^2 - \gamma_k^2 a_{3_k}^2}}\right]}{\sqrt{a_k^2 - \gamma_k^2 a_{3_k}^2}} \right\},$$

and

$$g_k(u) = \frac{2}{a_k^2 - \gamma_k^2 a_{3_k}^2} \left\{ \left(\gamma_k^2 a_{3_k}^2 + u\right)^{-1/2} + \frac{\tan^{-1}\left[\sqrt{\frac{\gamma_k^2 a_{3_k}^2 + u}{a_k^2 - \gamma_k^2 a_{3_k}^2}}\right]}{\sqrt{a_k^2 - \gamma_k^2 a_{3_k}^2}} \right\}.$$

We also have $u_{0_k}(x,y,z) = \lambda_k\left(x,y,z,m_0^2(s_k)\right)/m_0^2(s_k)$, and
$u_{1_k}(x,y,z) = \lambda_k\left(x,y,z,m_1^2(s_k)\right)/m_1^2(s_k)$, in which

$$2\lambda_k\left(x,y,z,m^2\right) = x^2+y^2+\gamma_k^2\left(z-\langle z\rangle_k\right)^2 - m^2a_k^2 - m^2\gamma_k^2a_{3k}^2 + \left[\left(x^2+y^2+\gamma_k^2\left(z-\langle z\rangle_k\right)^2 - m^2a_k^2 - m^2\gamma_k^2a_{3k}^2\right)^2 + 4m^2\gamma_k^2\left(a_{3k}^2\left(x^2+y^2\right) + a_k^2\left(\left(z-\langle z\rangle_k\right)^2 - m^2a_{3k}^2\right)\right)\right]^{1/2}.$$

If $\left(x^2+y^2\right)/a_k^2 + \left(z-\langle z\rangle_k\right)^2/a_{3k}^2 < m^2$, then $\lambda_k\left(x,y,z,m^2\right) = 0$.

Knowing the force per unit charge from a single shell, one can easily deduce the resulting total force acting on a given macroparticle by summing over all ellipsoidal shells s_k, and then over all momentum bins k:

$$\begin{aligned} F_x &= x\sum_k \frac{a_k^2 a_{3_k}}{\gamma_k}\sum_{s_k}\frac{\rho_{s_k}}{2\varepsilon_0}A_{s_k}, \\ F_z &= \sum_k\left(z-\langle z\rangle_k\right)\gamma_k\, a_k^2 a_{3_k}\sum_{s_k}\frac{\rho_{s_k}}{2\varepsilon_0}A_{3_{s_k}}. \end{aligned}$$

SIMULATION RESULTS

We have applied this method to two cases: (i) electron beams with $\eta \sim 100\%$ such as are produced with a SMLWFA injector and (ii) electron bunches with low η ($< 5\%$).

SMLWFA injector

As mentioned in the introduction, the density of the electron bunches produced by the SMLWFA scheme is two orders of magnitude greater that in the CPI scheme. The initial electron momentum spectrum is also much wider. Distributions well fitted by an exponential function have been observed experimentally, with an effective temperature kT greater than 2 MeV [6]-[11].

In Fig. 1, we plot the equivalent uniform-density bunch radius, bunch length, divergence, and relative momentum spread, as a function of propagation distance, for the SMLWFA case. The equivalent uniform-density quantities are obtained from the rms values by multiplication by $\sqrt{5}$. The initial phase-space density was assumed uniform in all 6 dimensions. The bunch charge is $Q = 1$ nC. The initial bunch longitudinal momentum ranges from $p_{z_i} : 0.1 \rightarrow 6$ MeV/c, corresponding to an exponential distribution with $kT_i = 2$ MeV. From Fig. 1, we see that space charge effects vanish at a very early stage (50-100 μm). Subsequent motion is dominantly ballistic.

Fig. 2 shows the longitudinal momentum spectrum of the bunch, initially and after 220 μm of propagation. The highly nonlinear space charge interaction results in the formation of a low energy tail shown in the figure.

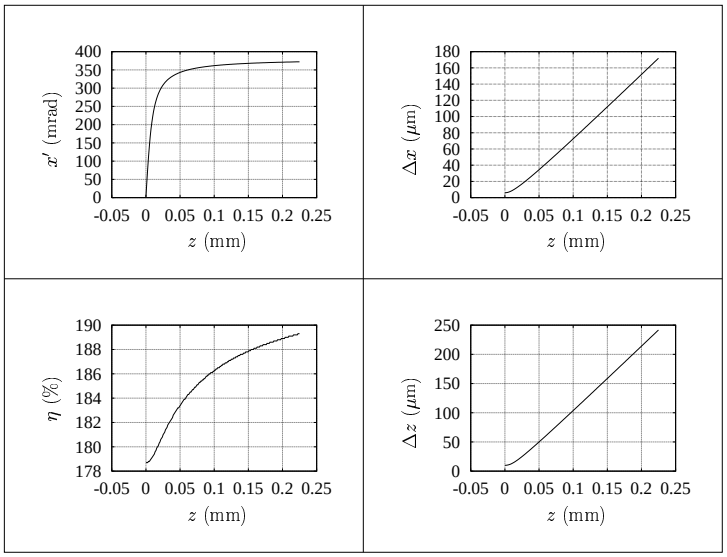

FIGURE 1. Equivalent uniform-density beam parameters as a function of propagation distance for the SMLWFA injector case. The top-left figure shows the bunch's divergence x', below it the relative momentum spread η, on the top-right the radius Δx and underneath it the bunch length Δz.

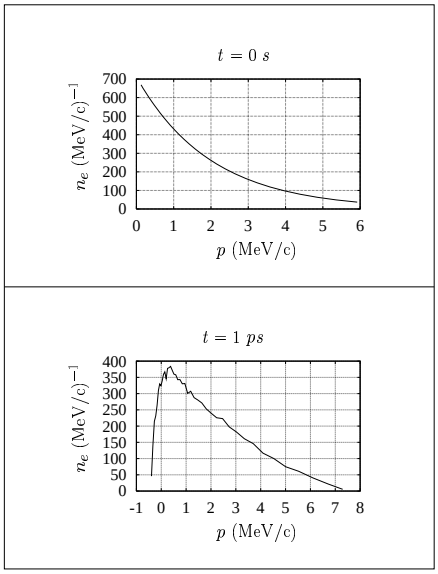

FIGURE 2. Longitudinal momentum spectrum of the bunch (electron energy density vs. p in MeV/c). The top figure shows the initial electron spectrum and the bottom one, the spectrum after 220 μm of propagation. The final distribution shows approximately 8% of backward electrons and a total energy gain on the order of 1 MeV, due to self acceleration. This same mechanism will result in emittance growth.

Fig. 3 shows the phase-space distribution of the bunch after 220 μm. Macroparticles have been color-coded to label the initial longitudinal momentum. Electrons that have an initial momentum greater than 5 MeV/c are shown in blue (black); low energy electrons with $p_z < 1$ MeV/c are shown in red (dark gray); the remaining electrons

are in green (light gray). The high energy electrons stay well collimated, while the low energy electrons, followed by backward particles, form a long tail and a transverse halo.

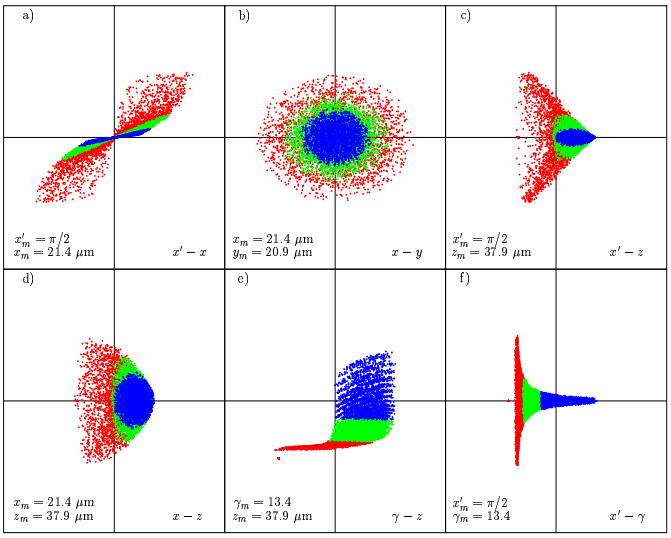

FIGURE 3. Phase-space plot of the bunch distribution function after 220 μm. The top-left figure (a) shows transverse phase-space $x' - x$, (b) a beam cross section $x - y$ and (c) divergence versus propagation distance $x' - z$. On the bottom-right (d), a beam side view $x - z$ is shown, (e) the longitunal phase-space $\gamma - z$ and (f) divergence x' versus γ. Electrons that have an initial momentum greater than 5 MeV/c are shown in blue (black); low energy electrons with $p_z < 1$ MeV/c are shown in red (dark gray); the remaining electrons are in green (light gray).

Low energy spread electron bunches

Colliding pulses

Typical electrons bunches produced by CPI's have a lower charge density and a higher average energy than in the SMLWFA regime. The blowout caused by the space charge forces is expected to be smaller than for SMLWFA injectors, which results in better beam quality.

In Fig. 4, we plot the equivalent uniform-density bunch radius as a function of propagation distance for the CPI example. The initial phase-space density was assumed again uniform in all 6 dimensions. The bunch charge is $Q = 1$ pC, the initial length $\Delta z = 2.5\ \mu$m, divergence $x' = 5$ mrad, energy spread $\eta = 2$ % and longitudinal momentum $\langle p_{z_i} \rangle = 30$ MeV/c. In this case space charge forces can be neglected and the bunch dynamics is purely ballistic.

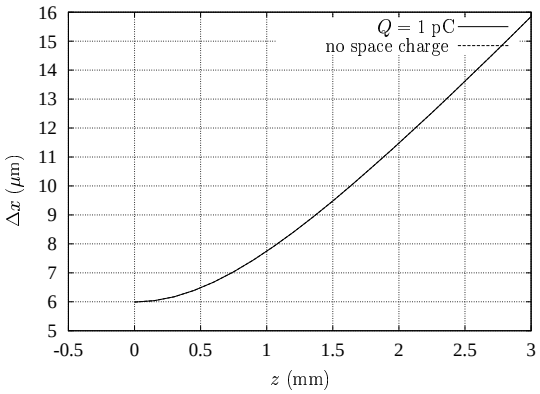

FIGURE 4. Equivalent uniform-density bunch radius as a function of propagation distance for the CPI case. $Q = 0$ (no space charge) and $Q = 1$ pC cases show a similar behavior.

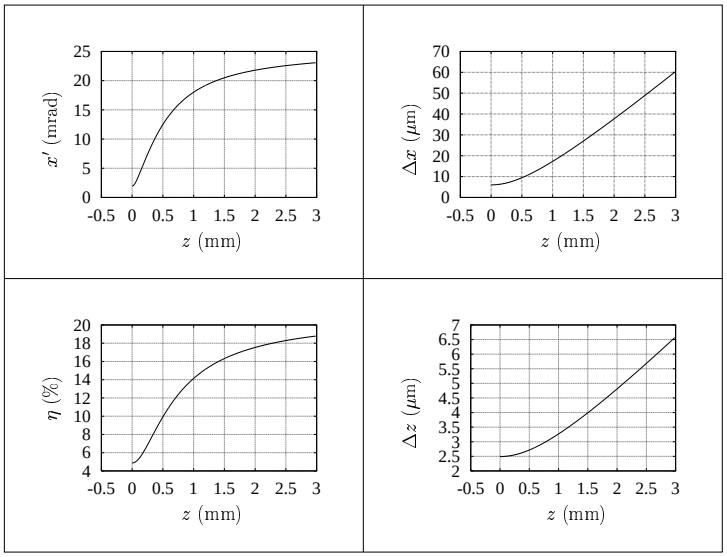

FIGURE 5. Equivalent uniform-density beam parameters as a function of propagation distance for a bunch with low energy spread. The top-left figure shows the bunch's divergence, below it the relative momentum spread, on the top-right the radius and underneath it the bunch length.

General case

The parameter values used in the example described here are slightly overestimated for simulation purposes; actual CPI's are expected to have a somewhat larger energy and a lower charge per bunch, resulting in smaller space charge forces.

In Fig. 5, the equivalent uniform-density bunch radius, bunch length, divergence, and relative momentum spread, as a function of propagation distance, is shown. The bunch charge is $Q = 20$ pC, and the initial bunch longitudinal momentum is $\langle p_{z_i} \rangle = 5.25$ MeV/c. After 3 mm of propagation the beam approaches the emittance dominated regime. The divergence and the relative momentum spread reach asymptotic values of

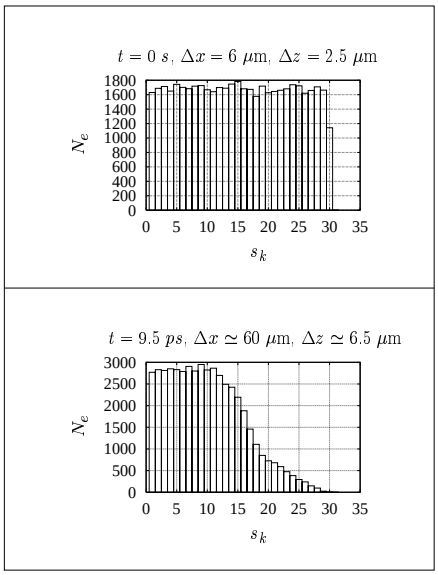

FIGURE 6. Histogram (number of electrons vs. shell index s_k) of a low energy spread bunch's transverse distribution (as measured by the density of the ellipsoidal shells), both initially and after 3 mm of propagation in vacuum.

20 mrad and 18.5%, respectively. The nonlinear nature of space charge force acting on the bunch makes the initial uniform density become non uniform as shown in Fig. 6. Wings and erosion can be seen clearly, which will lead to emittance growth [5].

CONCLUSION

Space charge effects are of important concern for electron beams produced in laser plasma experiments. Such beams are very compact, with a high charge density, a relatively low energy (up to a few tens of MeV), and a large energy spread. Conventional space-charge approaches, restricted to small energy spread beams, are not applicable in this case. In this paper, we have described a novel technique which uses an ellipsoidal model for the beam transverse distribution and allows the treatment of arbitrarily large energy spreads. This model has been used to study the six-dimensional evolution of the beam phase space for two examples relevant to beams produced in laser-plasma experiments. Large energy spread and short electron bunches, such as are produced by the SMLWFA regime, are expected to undergo an important space charge blowout due to the high charge density per bunch. On the contrary, beams produced by CPI's can propagate in vacuum without experiencing the detrimental effects of space charge because they have a somewhat higher average energy per bunch and a lower charge density.

ACKNOWLEDGMENTS

The authors acknowledge useful discussions with Brad Shadwick and Carl Schroeder. This work was supported by the U.S. Department of Energy, Contract No. DE-AC-03-76SF0098.

REFERENCES

1. For a review see, E. Esarey et al., IEEE Trans. Plasma Sci. **PS-24**, 252 (1996).
2. C.B. Schroeder et al., Phys. Rev. E **59**, 6037 (1999); E. Esarey et al., Phys. Rev. Lett. **79**, 2682 (1997).
3. G. Fubiani, W. Leemans and E. Esarey, in *Advanced Accelerator Concepts*, edited by P. Colestock and S. Kelly, AIP Conf. Proc. **569** (Amer. Inst. Phys., NY, 2001), pp. 423-435.
4. S. Chandrasekhar, *Ellipsoidal Figures of Equilibrium* (Dover Publications, 1969).
5. M. Reiser, *Theory and design of charged particle beams* (Wiley, 1994).
6. A. Modena et al., Nature **377**, 606 (1995); D. Gordon et al., Phys. Rev. Lett. **80**, 2133 (1998).
7. K. Nakajima et al., Phys. Rev. Lett. **74**, 4428 (1995).
8. D. Umstadter et al., Science **273**, 472 (1996); R. Wagner et al., Phys. Rev. Lett. **78**, 3125 (1997).
9. A. Ting et al., Phys. Plasmas **4**, 1889 (1997); C.I. Moore et al., Phys. Rev. Lett. **79**, 3909 (1997).
10. W.P. Leemans, et al., Phys. Plasmas **8**, 2510 (2001)
11. V. Malka et al., Phys. Plasmas **8**, 2605 (2001);